PALEOCEANOGRAPHY, VOL. 17, NO. 2, 1025, 10.1029/2001PA000639, 2002

Arctic ice export events and their potential impact on global climate during the late Pleistocene

Dennis A. Darby and Jens F. Bischof
Department of Ocean, Earth, and Atmospheric Sciences, Old Dominion University, Norfolk, Virginia, USA

Robert F. Spielhagen
GEOMAR Research Center for Marine Geosciences, Kiel, Germany

Steven A. Marshall and Stephen W. Herman
Department of Ocean, Earth, and Atmospheric Sciences, Old Dominion University, Norfolk, Virginia, USA

Received 8 March 2001; revised 26 October 2001; accepted 30 November 2001; published 14 June 2002.

[1] Ice sheets in the North American Arctic and, to a lesser extent, those in northern Eurasia calved large quantities of icebergs that drifted through Fram Strait into the Greenland Sea several times during the late Pleistocene. These icebergs deposited Fe oxide grains (45–250 μm) and coarse lithic clasts >250 μm matched to specific circum-Arctic sources. Four massive Arctic iceberg export events are identified from the Laurentide and the Innuitian ice sheets, between 14 and 34 ka (calendar years) in a sediment core from Fram Strait. These relatively short duration (<1–4 kyr) events contain 3–5 times the background levels of Fe oxide grains. They began suddenly, as indicated by a steep rise in the number of grains matched to an ice sheet source, suggesting rapid purges of ice through Fram Strait, due perhaps to collapse of ice sheets. The larger events from the northwestern Laurentide ice sheet are preceded by events from the Innuitian ice sheet. Despite the chronological uncertainties, the Arctic export events appear to occur prior to Heinrich events. *INDEX TERMS:* 4207 Oceanography: General: Arctic and Antarctic oceanography; 4215 Oceanography: General: Climate and interannual variability (3309); *KEYWORDS:* Arctic Ocean, ice-rafted detritus, paleoclimate, Fe oxide minerals, deglaciation, Heinrich events

1. Introduction

[2] Ice export from the Arctic Ocean to the Greenland Sea and North Atlantic has been recognized as an important factor influencing the formation of North Atlantic Deep Water (NADW) [*Aagaard and Carmack*, 1989; *Oppo and Lehman*, 1995; *Bischof and Darby*, 1997]. When this ice export increases, the surface salinity in these sub-Arctic seas and likewise the deep water formation decrease. This and the increased albedo effect caused by more ice in these seas should cause cooling according to current models [*Mysak and Venegas*, 1998]. While there are very few icebergs exiting Fram Strait today, the modern sea ice export through Fram Strait is significant and highly variable [*Kwok and Rothrock*, 1999]. In contrast to the present-day situation, not much is known about the extent of late Pleistocene glacial Arctic Ocean ice export through this important gateway. Here we will demonstrate that (1) sudden, massive iceberg calving events occurred in the North American Arctic ice sheets, (2) these events led to large quantities of glacial ice drifting through Fram Strait, and (3) these ice-rafting events most likely preceded the North Atlantic Heinrich events. Our findings shed new light on ice sheet behavior and point to the possibility that a direct link exists between sequential ice sheet disintegration, changes in the iceberg drift through Fram Strait into the sub-Arctic seas, and perhaps the cold parts of the Dansgaard-Oeschger cycles.

2. Methods

[3] We trace ice-rafted debris (IRD) in glacial marine sediments back to its sources by comparing every sample's composition with those of 310 circum-Arctic source area samples with discriminant function analysis (DFA) [*Darby and Bischof*, 1996]. The source area samples are shallow marine sediments and glacial tills that closely represent nearby bedrock formations. The source samples form 38 groups of unique petrographic and chemical composition (Figure 1). Each of these groups represents a possible source of iceberg and/or sea ice-rafted debris. Two different kinds of data were generated and used for DFA: (1) the petrographic and mineralogic composition of rock and mineral fragments >250 μm and (2) the chemical composition of individual Fe oxide grains in the 45–250 μm grain size fraction.

[4] All samples were split at 45, 63, and 250 μm. Fe oxide grains were magnetically separated from the 45–250 μm fraction and mounted in clear epoxy plugs, whose surface was ground to expose cross sections of the grains, then polished for ore microscopy and electron microprobe analyses. Nine different Fe oxide mineral types were identified and confirmed by chemical composition. Our chemical fingerprinting technique uses 12 elements in nine Fe oxide minerals to match individual grains to their source areas. Each grain must be closer to the source mineral composition

0883-8305/02/2001PA000639

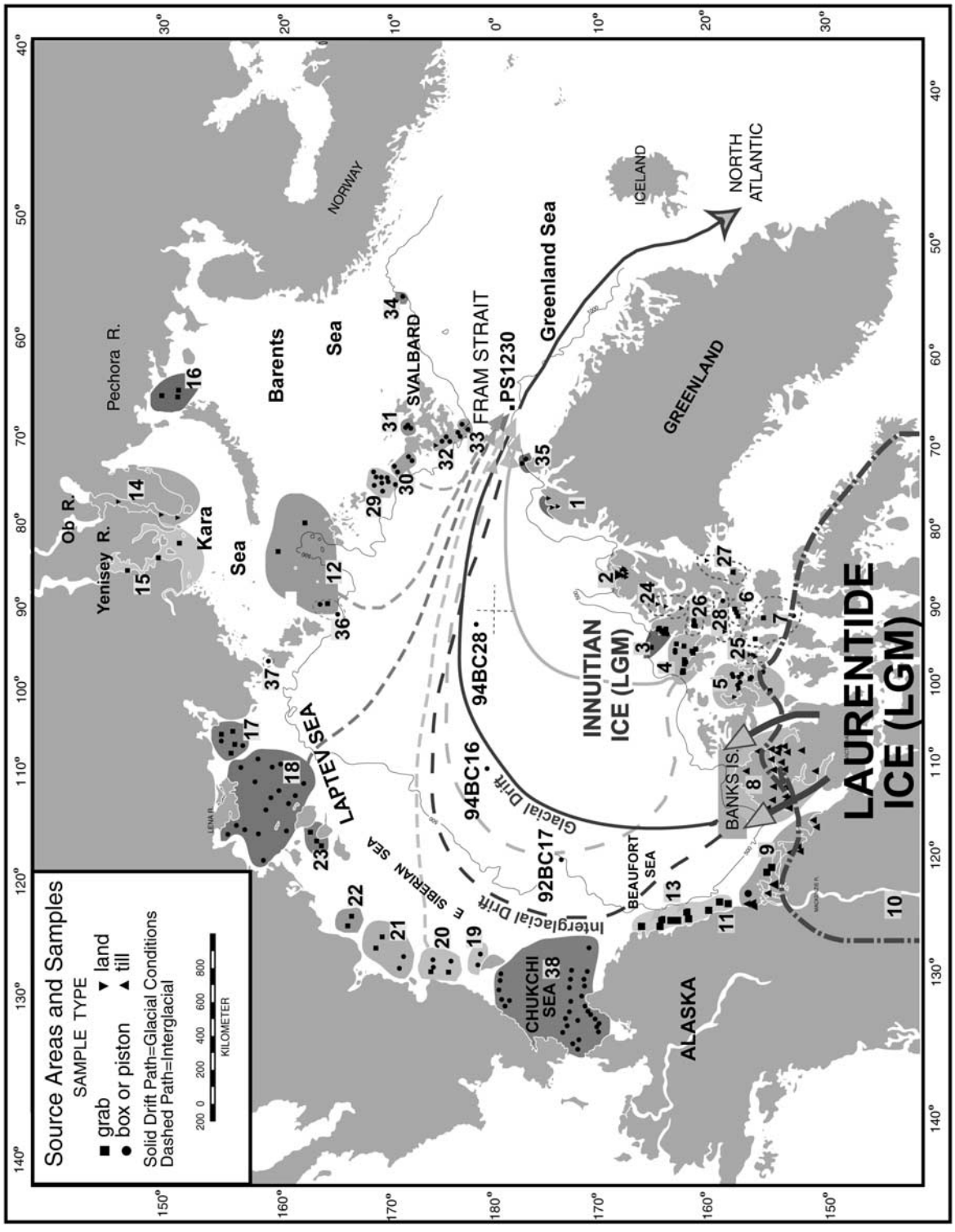

Figure 1. Circum-Arctic source areas (1–38) defined by unique source compositions and drift paths of icebergs from Arctic Laurentide ice sheet and Innuitian ice sheet to Fram Strait (solid drift paths) and the location of box core PS1230. Dashed drift paths of sea ice in the Arctic show the influence of the Beaufort Gyre during warmer intervals like the Holocene by displacing North American ice drift paths westward [after *Bischof and Darby*, 1997].

Table 1. AMS Radiocarbon Dates From Box Core PS1230

Depth, cm	Depth Interval	Age, ^{14}C years (^{13}C Corrected)	Age, ^{14}C years (Reservoir Corrected. −400 yr)	SD, ^{14}C years	Laboratory Number
0.5	0–1	2525	2125	75	ETH 9294
10.5	10–11	7880	7,480	90	ETH 9295
14.5	14–15	10870	10,470	110	ETH 9296
16.5	16–17	13180	12,780	120	ETH 9297
20.5	20–21	16160	15,760	230	AAR 1197
20.5	20–21	16130	15,730	140	ETH 9298
20.5	20–21	16140	15,740	120	Avg
24.5	24–25	16160	15,760	140	ETH 9299
24.5	24e25	16420	16,020	170	AAR 1198
24.5	24–25	16270	15,870	110	Avg
29.5	29–30	20080	19,680	250	AAR 1199
34.5	34–35	22290	21,890	210	ETH 9300
35.5	35–36	23100	22,700	360	AAR 1200
44.5	44–45	28830	28,430	350	ETH 9301

group centroid than half of the grains comprising that source group. This conservative criterion insures precise matches and prevents forced matches [*Darby and Bischof*, 1996], but it does result in no matches for about half of the analyzed grains. Only grains that were reliably matched to their sources are considered here.

[5] The composition of the >250 μm IRD was determined by counting 400–600 grains per sample on a counting tray under a binocular microscope at 40 times magnification. More than 300 different grain types are distinguished and grouped into 80 variables for DFA analysis [*Darby and Bischof*, 1996].

[6] The combined use of the 45–250 μm Fe oxides and the >250 μm grain petrography and mineralogy has these advantages: (1) a relatively large portion of the bulk sediment is traced to its sources; (2) the coarse grain petrography provides means of cross validation of the Fe oxide matches; (3) in addition to identifying a major source area for every sample with the >250 μm fraction, several other contributing sources can be identified by DFA of the individual Fe oxide grains.

3. Results

3.1. Physical Setting, Sediments, and Stratigraphy of Fram Strait Core PS1230

[7] Box core PS1230 is located in 1235 m water depth at 78.9°N, 4.8°W in Fram Strait (Figure 1), the major gateway between the Arctic and the global ocean. Ninety percent of the modern sea ice drifts through Fram Strait between 0° and 10°W (T. Vinje et al., Ice fluxes through Fram Strait, 1998, available at http://www.gfi.uib.no/~svein/esop2tv.html). Today, the core site is ice covered year-round and has low biologic productivity [*Bauch et al.*, 2001].

[8] The sediment is glacial marine, silty to sandy and gravelly mud. The top 10 cm have the lowest concentrations of coarse IRD and increased amounts of microflora and microfauna remains (mostly foraminifera shells). The lower part of the core is visibly layered and consists of sandy to gravelly mud with abundant coarse IRD, including centimeter-sized dropstones, and less microfossils than the top. The sediment sequence is similar to those from much of the Norwegian Greenland and Iceland seas [*Henrich et al.*, 1989]. In the lower Pleistocene portion of the core, the concentrations of coarse, ice-rafted rock and mineral grains vary from 1000 to 13,000 grains in ~35 cm^3 sediment volume. This variability suggests that a combination of any of the three following factors changed considerably during the Pleistocene: (1) the amounts of icebergs and sea ice that drifted across the site, (2) the IRD concentration in the drifting ice, or (3) the intensity of melting.

[9] The chronology in PS1230 and other cores in this study is provided by accelerator mass spectrometry (AMS) ^{14}C on the dominant planktonic foraminifera (*N. pachyderma,* synistral) (Table 1). Calibrated calendar ages and 1 σ age ranges for radiocarbon ages <20 kyr were calculated using the intercept method of CALIB REV, version 4.1.2 [*Stuiver and Reimer*, 1993] with the data set from *Stuiver et al.* [1998]. For radiocarbon ages >20 kyr, age shifts and uncertainty envelopes were obtained from *Voelker et al.* [1998]. At 20 ka, the offset of both methods is <200 years.

[10] The average sedimentation rate in PS1230 is 1.4 cm/kyr but varies from slightly less than 1 to nearly 5 cm/kyr. Sampling was continuous at 1 cm intervals, providing more than one sample per thousand years, except between 10 and 14 ka, where sedimentation rates are lower. The interval 20–25 cm is well dated (Table 1) and covers only ~1000 calendar years (18–19 calendar kyr), as interpolated from the dates in this core interval (Figure 2). Because of the variable sedimentation rates in this and other Arctic cores studied, age models use separate interpolations for each straight line segment of the radiocarbon measurements versus core depth [*Andrews*, 1998a]. Bioturbation is minimal, and mixing is restricted to a few centimeters on the basis of sediment layers with sharp boundaries (Figure 2) and comparison to nearby cores with 2–3 cm mixing depths [*Jones and Keigwin*, 1988].

3.2. IRD Composition

[11] The IRD >250 μm consists of a highly diverse assemblage of quartz grains and fragments of sedimentary, igneous, and metamorphic rocks in variable proportions. In all, 206 different IRD lithologies were found, of which up to 72 are present in every sample. The diversity of IRD is higher than in most samples from the Arctic Ocean [*Bischof*, 2000; *Bischof et al.*, 1996; *Bischof and Darby*, 1997],

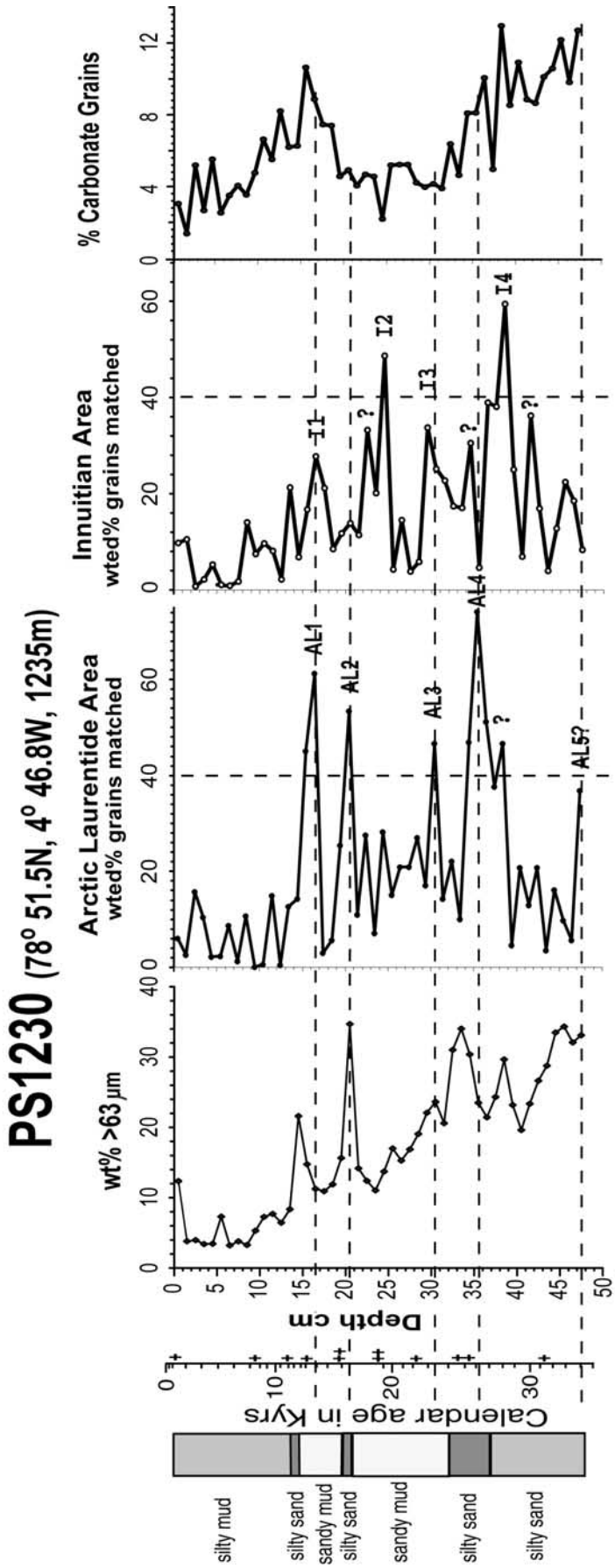

Figure 2. Arctic Laurentide (AL) and Innuitian (I) IRD events based on detrital Fe oxide mineral grain compositions matched to source area 8 on Figure 1 and source areas 2–7 plus 24–28, respectively.

indicating that a multitude of sources contributed to every sample. Carbonate fragments similar to those in till samples from Banks and Victoria Islands indicate a pervasive influence from the North American side of the Arctic Ocean, where vast expanses of carbonates exist. By contrast, the Eurasian side has only few and small carbonate exposures. In our source area data set the average carbonate percentage among >250 μm grains from Eurasia is 2.5%, but in core PS1230, carbonates are 2–13%. For most of the Pleistocene section, carbonates are significantly higher than 2%, which requires a contribution from the North American Arctic or from north Greenland.

[12] DFA determined that some of the IRD came from the Queen Elizabeth Islands, primarily Axel Heiberg, Ellesmere, and Ellef Ringnes Islands, which were covered by the Innuitian ice sheet during the Pleistocene [*Dyke*, 1999; *England*, 1999; *O'Cofaigh et al.*, 2000]. Other sources of coarse IRD include the southwestern Canadian Arctic Archipelago, primarily Victoria and Banks Islands and the Mackenzie District, an area that was buried under the northwestern, Arctic-facing Laurentide Ice sheet [*Dyke et al.*, 1989], and to a lesser extent, also from Svalbard, Franz Josef Land, and the Kara Sea. A direct variable-by-variable comparison between each of the 80 variables for the sample and the data range of the same variable in the DFA-determined source revealed that while DFA identified a major source, as much as 30% of the coarse IRD came from other sources. These additional sources are revealed by the DFA results on the geochemistry of individual Fe oxide grains.

[13] Verification of the DFA results is also possible in certain instances because of the presence of very unique lithologies among the >250 μm grains. The bottom 15 cm of the PS1230 sequence of coarse IRD were mostly assigned by DFA to the northern Queen Elizabeth Islands. They contain tiny fragments of a very conspicuous and rare rock type, a multicolored, low-grade phyllite with randomly oriented amphibole blades. The only other place where these rocks occur is in two piston cores from north of Ellesmere Island, core FL-561 [*Bischof et al.*, 1996] and FL-542 [*Bischof and Darby*, 1997]. M. Bjørnerud (unpublished technical report, 1986) describes this rock type from Yelverton Inlet, northwestern Ellesmere Island.

[14] The IRD composition reveals details about the paleo-ice drift that complement and extend the capabilities of DFA. In most Arctic Ocean IRD assemblages from cores with abundant (up to 52%) detrital carbonate, these are dominated by white and tan colored types, with far fewer gray and yellow ones. At the PS1230 site, not only is the overall abundance of carbonates diminished, indicative of significant dilution of the North American coarse IRD due to addition of icebergs with noncarbonate lithologies along the drift path, but also their color distribution has changed. Instead of white and tan carbonates, here gray carbonates are most abundant, followed by white, with occasional brown types. In tills from Banks and Victoria Islands, white carbonates are most abundant and outnumber brown varieties by a factor of three. Quite conceivably, these carbonates are derived from various carbonate terrains besides Victoria Island, such as parts of the Queen Elizabeth Islands or north Greenland.

[15] That some of the IRD sources include north Greenland is evident from volcanic rock fragments. Although they occur in small percentages, volcanic rock fragments are much more frequent in PS1230 than in the Arctic Ocean [*Bischof et al.*, 1996; *Bischof and Darby*, 1997] and occur in a variety of different colors. The closest volcanic rock exposure to the core site is the Kap Washington volcanics in northeast Greenland [*Escher and Watt*, 1976]. In theory, the volcanics could have also come from Franz Josef Land [*Okulitch et al.*, 1989], but the volcanic rocks in core PS1230 are multicolored, whereas those from Franz Josef Land, represented in our source data set (Figure 1), are uniformly medium to dark green basalts. Therefore the origin of the volcanic rocks is northeast Greenland.

3.3. Fe Oxides in Fram Strait Sediment

[16] The quantities of ice-rafted Fe oxide mineral grains in the 45–250 μm fraction vary considerably, from 14 to 130 grains per sample (mean of 64). Like the coarse IRD, these grains decrease from an average 71 grains per sample in the late Pleistocene to 44 per sample in the Holocene. The number of Fe oxide grains matched to a source decrease from an average 41 per sample to 32 per sample in these same intervals. Some samples contain fewer than 20 grains matched to all sources using our conservative criteria. Because insignificant and misleading peaks in the percentages of these grains matched to any one source can result where grain numbers are very low, we use a weighted percentage. This value is calculated by multiplying the percent matched to a source by one tenth of the number of grains matched to this source. Thus source percentages based on far fewer than 10 grains are decreased while the opposite is true for percentages based on far more than 10. Weighted Fe oxide peaks therefore reflect both the grain frequencies and the relative proportion from specific sources.

[17] Analyses of Fe oxide grains found in sea ice floes from well-constrained source areas indicate that extraneous sources, if present, always are comprised of fewer than ~5 grains [*Darby and Bischof*, 1998]. For the weighted percent we divide by 10 instead of 5 to insure that peaks in Fe oxide grain percents are based on >5–10 grains. Fe oxide peaks are herein defined as weighted percents >25–30% and >10% above background. The Fe oxide grain peaks matched to Banks and Victoria Islands (source area 8, Figure 1) were compared to peaks in unweighted percents, which closely coincide with weighted percent peaks (AL peaks, Figure 2) except for one instance at 27–28 cm, where only 12 grains were matched to sources. All unweighted peaks matched to this source were 30–40%, and background values were <10–20%.

3.4. IRD Events Recorded at Fram Strait Site

[18] Significant, rapid fluctuations in the percentages of Fe oxide grains from different sources occurred during the last 34,000 years (Figure 2). A major source of IRD was the northwestern Laurentide ice sheet that calved into the Arctic Ocean, herein referred to as the Arctic Laurentide Ice Sheet (ALIS). The ALIS is recognized as a source because the elemental composition of detrital Fe oxide grains in PS1230 precisely matches those in the tills of Banks and Victoria

Islands. Another important indicator of the ALIS source is the presence of light-colored detrital carbonate, which is relatively abundant in ALIS tills and derived from the extensive Paleozoic carbonates exposed on Victoria Island [*Bischof et al.*, 1996]. All of the ALIS Fe oxide grain peaks in PS1230 occur in intervals with $\geq$4% detrital, light-colored carbonate, and two ALIS peaks (1 and 4) coincide with peaks of >8% detrital carbonate (Figure 2).

[19] Another important but secondary source of Fe oxide grains in this core is the Innuitian ice sheet (IIS) in the northern Canadian Islands (source areas 2–7 and 24–28 on Figure 1). These grains match to tills and surface sediments from these islands and the intervening channels and shelves [*Bischof and Darby*, 1999].

[20] In PS1230 the ALIS and IIS Fe oxide peaks are only 2–5 cm thick and <1–4 kyr in duration. Between 18 and 19 ka in PS1230, there occurs a peak in Fe oxide grains from ALIS (19–21 cm) and a peak from the Innuitian ice sheet (22–25 cm). Even given the errors in radiocarbon dating and interpolated ages for this interval (Table 1), it is difficult to extend the duration of these two separate peaks to much more than a thousand years. Other peaks have similar trends but do not occur in core intervals with high enough sedimentation rates to constrain their duration as well as peaks AL2 and I2 (Figure 2).

[21] Similar Fe oxide grain peaks from the ALIS occur in cores from the western Arctic Ocean to Fram Strait (Figure 3). While these Arctic cores have generally low and highly variable sedimentation rates [*Darby et al.*, 1997], the Fe oxide grain peaks from the ALIS occur at about the same time in several of these cores. For example, peak AL1 coincides with the beginning of the "Holocene" increase in foraminifera abundance in these cores [*Darby et al.*, 1997]. The interpolated calendar ages for these peaks vary between 13 and 15 ka. The large range in ages is most likely due to mixing and low resolution, but in 92BC17 this rise in foraminifera occurs above a barren zone where large volume samples (>100 cm^3) failed to find even a single foraminifer. The radiocarbon age 2 cm above this initial rise in foraminifer abundance is 12.4 ka [*Darby et al.*, 1997] or 14.4 calendar kyr B.P. and probably represent a minimum age because no foraminifera could be mixed in from below to increase the age of this event. This age is close to the radiocarbon calibrated age for this event in PS1230 (15.3 calendar kyr B.P.). Thus the age of the AL1 peak is probably closer to 15 calendar kyr.

[22] Surprisingly, the relatively close northern Greenland ice sheet did not supply greater quantities of Fe oxide IRD than the ALIS and IIS sources to the location of PS1230 over the last 17 kyr (Figure 4). These data demonstrate that nearby sources can be distinguished from very distant ones and that nearby sources in some cases do not overwhelm the distant signal. Although the Fe oxide grain peaks matched to northern Greenland are lower in amplitude than ALIS or IIS peaks, all but one of these Greenland peaks coincide with peaks from the ALIS (Figure 4).

[23] Beginning at ~14 ka, decreasing North American IRD is surpassed by increasing amounts of IRD from sources in the Russian Arctic (Figure 5). The largest percentage of Fe oxide grains from the Holocene match to the Kara and Laptev Seas. Several Fe oxide peaks from these two large Russian shelves occur at the same time. The increase of Russian Arctic IRD is accompanied by synchronous increases in the amounts of chert and quartz among the >250 μm IRD, matching the abundance of these lithologies in the Laptev and Kara Seas.

4. Discussion

4.1. Iceberg Versus Sea Ice Rafting

[24] During the last 10 kyr the weight percentages of the >63 μm fraction are <4% (Figures 2 and 5), suggesting transport by sea ice rather than iceberg rafting [*Pfirman et al.*, 1989; *Reimnitz et al.*, 1998; *Nürnberg et al.*, 1994]. The increase in Fe oxide grains from unglaciated Russian shelves such as the Laptev Sea supports sea ice rafting as the most important transport process during the Holocene. Icebergs are rare in the Arctic Ocean today and probably were for most of the Holocene.

[25] Fe oxide grain matches to the Arctic Laurentide and Innuitian areas during the Holocene must also be due to sea ice rafting because numerous radiocarbon dates on marine molluscs place the retreat of the Arctic ice sheets onto land positions to sometime between 10 and 9 ka [*Dyke*, 1999; *Dyke et al.*, 1992], after which iceberg rafting was not possible. Along the Canadian arctic coast, sea ice can entrain and transport glacial sediment in three important ways: erosion of coastal cliffs composed of glacial tills, fast ice in the coastal areas, and suspension freezing on the shallow shelves (water depths <50 m), which contain detrital grains reworked from terrestrial glacial deposits [*Bischof and Darby*, 1999; *Reimnitz et al.*, 1987]. Peaks older than 10 ka from the ALIS and IIS represent primarily iceberg transport on the basis of the abundance of coarse IRD in the Pleistocene section and on the similarity of the IRD grain size distribution to glacial tills.

[26] During the late Pleistocene, Fe oxide peaks from the ALIS and IIS rarely coincide with peaks in the overall abundance of coarse IRD (Figure 2). This suggests that the Fe oxide peaks are independent from fluctuations in the delivery of coarse IRD. In other words, the percentage of Fe oxide grains matched to the ALIS indicates the input from this source relative to all other sources and not the delivery of coarse IRD to the seafloor at this Fram Strait core site.

4.2. IRD Events and Ice Sheet Dynamics

[27] The abundance of coarse IRD in PS1230 is a function of (1) the quantity of icebergs and sea ice that drifted across the site, (2) the entrained sediment load, (3) the melt out rate, and (4) the drift paths. The surface water temperature largely controls melt out rates. At present, this temperature is close to the freezing point most of the year, limiting the melt out rate of debris from drifting ice to a minimum [*Hebbeln and Wefer*, 1991]. Generally low basal melting rates are also confirmed by very low sedimentation rates in the Arctic Ocean [*Clark et al.*, 1980, 1986; *Stein et al.*, 1994; *Darby et al.*, 1997] and by the fact that some IRD survived >3000 km of drift without being lost before the arrival at the core site. At the same time, the presence of

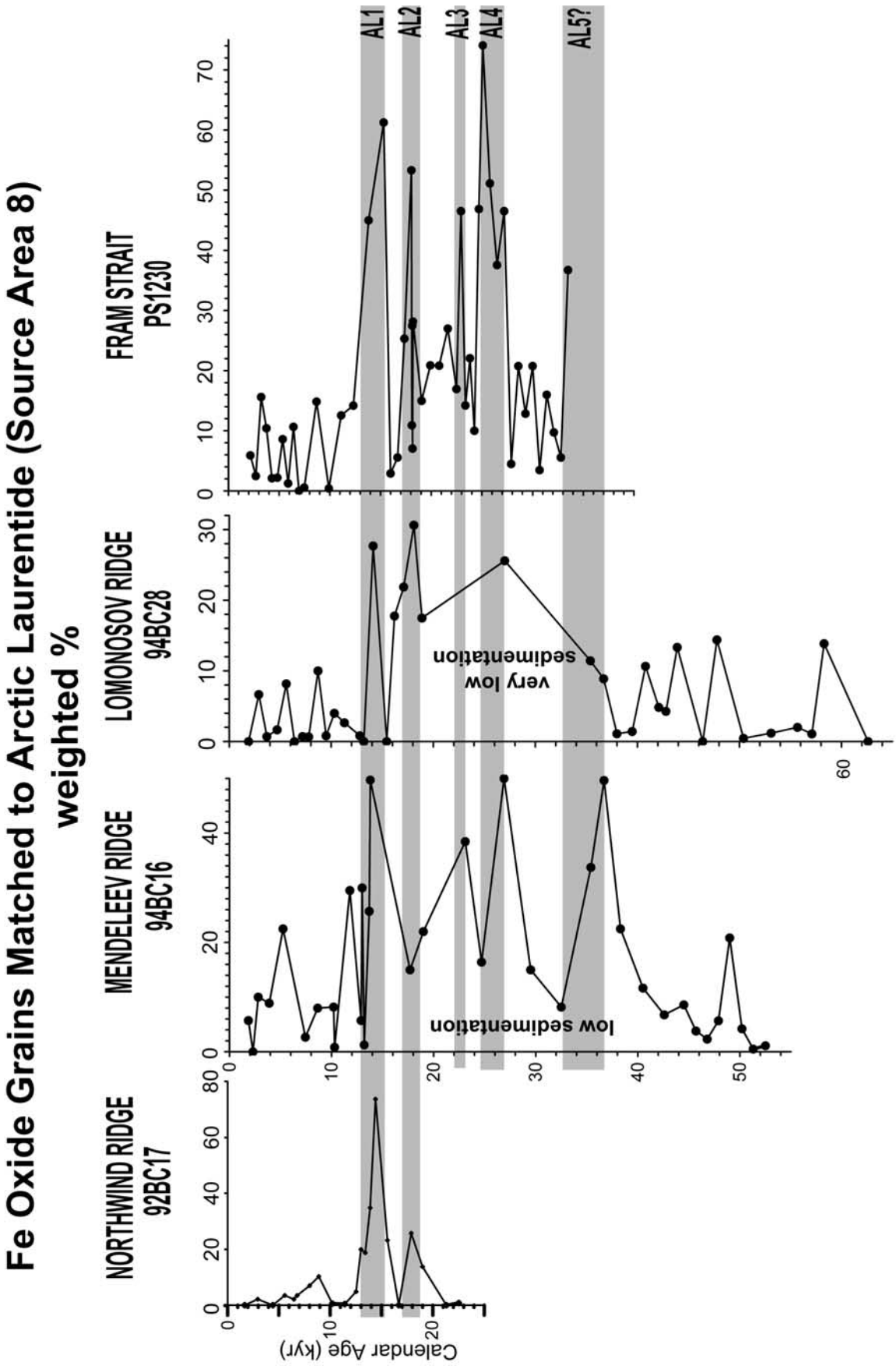

Figure 3. Correlation of Arctic Laurentide Fe oxide peaks in box cores across the Arctic Ocean (Figure 1). Radiocarbon age models used for these correlations are from *Darby et al.* [1997] and *Poore et al.* [1999].

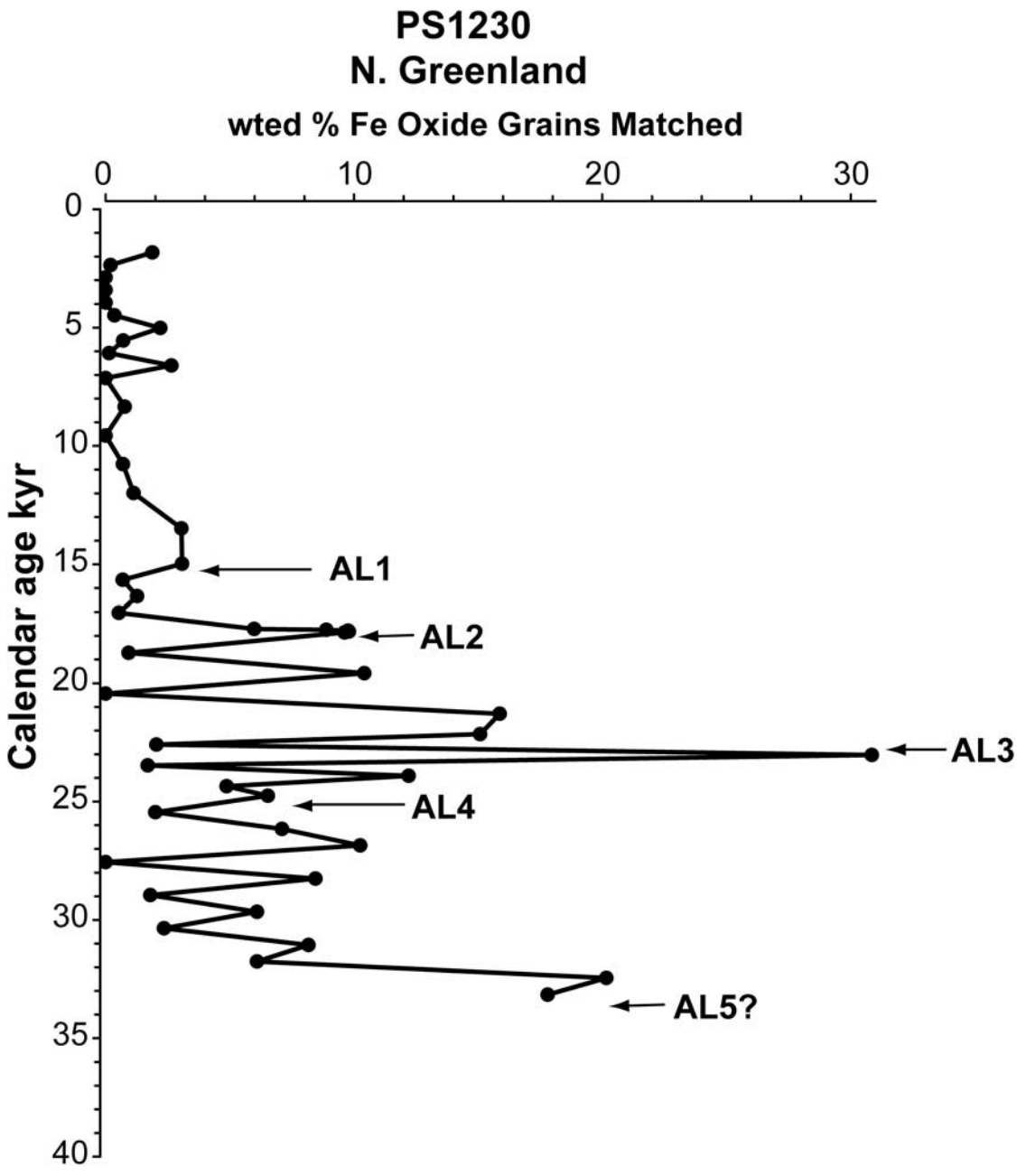

Figure 4. Fe oxide grains matched to northern Greenland in the Fram Strait core, which display smaller peaks compared to ALIS events (1–5) but occur at nearly the same time as many of the ALIS peaks in Figure 2.

ALIS Fe oxide peaks in several cores along this 3000 km drift track (Figure 1) suggests large numbers of icebergs. The location of PS1230 is north of the present sea ice margin, and this front was much farther south in the late Pleistocene [*Ruddiman*, 1977; *Bischof*, 2000]. All drift paths are constrained at the relatively narrow Fram Strait core site. Thus the relative strength of IRD delivery to this location was controlled by the quantity of ice drifting overhead and differences in the amount of entrained IRD and not by changing melt out rates or drift paths [*Dowdeswell and Dowdeswell*, 1989; *Dowdeswell and Murray*, 1990; *Warren*, 1992; *Dowdeswell et al.*, 1995]. The rapid onset and relatively short duration of the Fe oxide grain peaks suggest massive and fast deglaciation in parts of the ALIS and IIS, producing large quantities of icebergs.

4.3. Magnitude of Arctic Laurentide Ice Sheet IRD Events

[28] To estimate the quantity of icebergs that calved into the Arctic Ocean during one of the ALIS IRD events, we

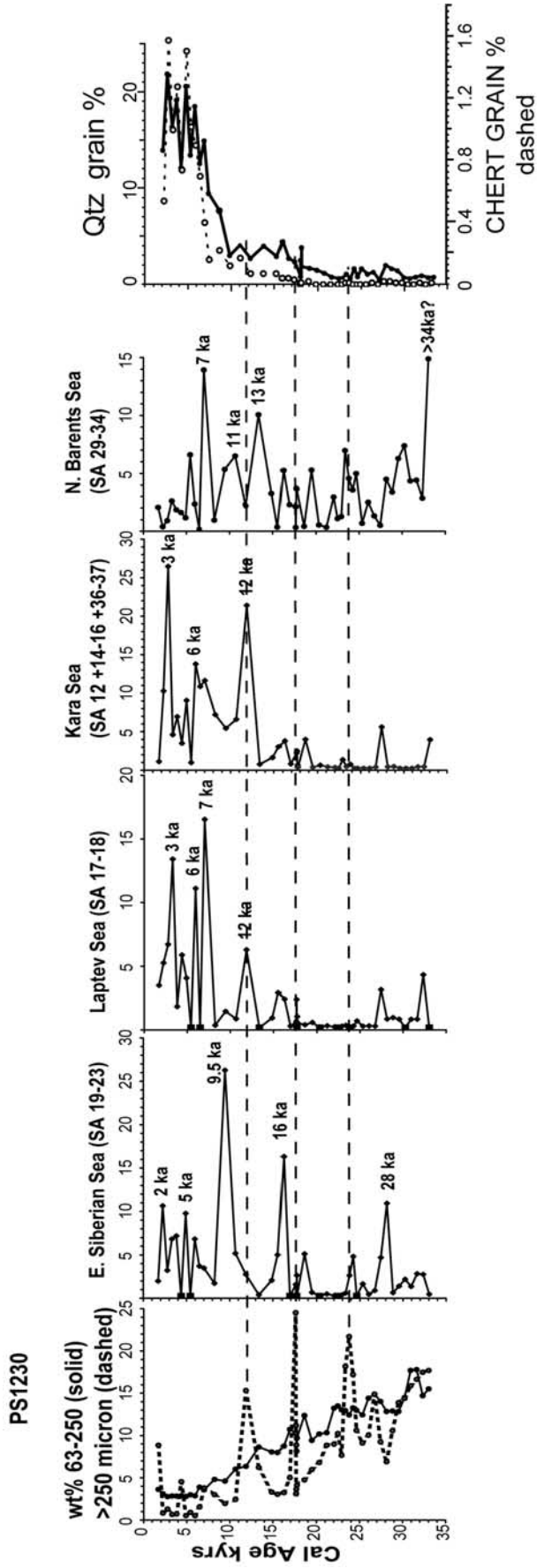

Figure 5. IRD events originating from Russian shelves increase in frequency and amplitude in the last 13,000 years. Rarely do these occur at peaks in coarse IRD.

use the proportion of Fe oxide grains in PS1230 matched to this ice sheet, assuming that the increase in grains matched to the ALIS is proportional to the increase in iceberg flux through Fram Strait. The area of the ALIS that flowed into the Arctic Ocean is $\sim 1.5 \times 10^6$ km^2 [*Clark et al.*, 1996]. Using the Laurentide reconstruction of 18 ka from *Clark et al.* [1996], ALIS had a volume of $\sim 1.3 \times 10^6$ km^3, which disappeared between 18 and 10 ka [*Dyke*, 1987]. Allowing for ~20% loss by mass wasting in situ and adding ~4 cm of ice per year over the 8000 years during glacial times based on 10 cm/yr ice accumulation in northern Greenland today, a maximum of $\sim 1.5 \times 10^6$ km^3 of icebergs could have calved from this ice sheet during the 8000 year long deglaciation. During this time, two IRD events occurred, AL1 and AL2 (Figure 2). If they lasted <1.5 kyr, then each IRD accounts for 19% of this 8 kyr interval. During these events, 3 times as many grains came from the ALIS than during the lows in between (using unweighted percents). Thus the two IRD events accounted for ~64% of the total ice that calved from the ALIS during this 8 kyr interval, or a maximum of 10^6 km^3. This amounts to an annual flux of fresh water bound in glacial icebergs of 350 km^3/yr through Fram Strait during an ALIS IRD event. The icebergs added ~15% to the present-day average annual sea ice volume flow through Fram Strait [*Kwok and Rothrock*, 1999]. More importantly, the icebergs would have survived longer and melted farther south than sea ice with a potentially significant impact on deep water production. For comparison, the range of estimates for iceberg flux through Hudson Strait during a Heinrich event is 312–2800 km^3/yr [*Dowdeswell et al.*, 1995; *MacAyeal*, 1993].

[29] Our estimate is conservative. If the actual values for the annual ice sheet thickness growth rate were larger and the duration of the iceberg pulses were shorter than our estimates, the amount of glacial ice that drifted through Fram Strait at times during the Pleistocene could have been considerably higher than our estimate, perhaps exceeding 1000 km^3/yr. Recent findings of plough and gouge marks at nearly 1000 m water depth on the Lomonosov Ridge and ~700 m on the Chukchi Borderland areas suggest that large ice shelves once existed in the Arctic [*Polyak et al.*, 2001]. Using a somewhat different approach, *Bischof* [2000] obtained an average volume flux of icebergs through Fram Strait of 270 km^3/yr (freshwater equivalent) with a range of 180-530 km^3/yr. Adding the volume flux of sea ice, the total freshwater flow during a deglaciation event was 3870 km^3, with a minimum flux of 3780 km^3 and a maximum of 4130 km^3 per year [*Bischof*, 2000]. Using these larger ice volume estimates, the amount of freshwater that was delivered from the Arctic Ocean to the sub-Arctic seas during the late Pleistocene by sea ice and glacial icebergs was up to 65–80% larger than at present.

4.4. Stratigraphic Relationship Between Arctic Laurentide and Innuitian IRD Events

[30] Some Fe oxide grain peaks from the IIS and the ALIS occur at about the same depth intervals in PS1230 (Figures 2 and 6). Where the resolution allows, for instance, at ALIS events 2–4, the Innuitian IRD events precede each Arctic Laurentide event by ~1–1.5 kyr. Where an Innuitian peak (e.g., I1) nearly coincides with an ALIS peak, the Innuitian Fe oxide grain IRD event begins to rise prior to the ALIS event and peaks just prior to the ALIS event (Figure 6). All four ALIS events exceed 40% of grains, while only two of the Innuitian Fe oxide grain events are above this arbitrary level (Figure 2). Obviously, the ALIS events are larger, as might be expected from the magnitude of the Laurentide ice sheet compared to the Innuitian ice sheet. Where the IIS events are largest (>40%), they clearly precede ALIS events immediately above stratigraphically (Figure 6).

[31] The stratigraphic relationship between ALIS and IIS Fe oxide grain peaks is more difficult to interpret in the cores from the central Arctic Ocean because the Innuitian icebergs followed different drift paths than the ALIS icebergs (Figure 1) [*Bischof and Darby*, 1997]. Thus Innuitian icebergs did not always reach the locations of the other Arctic Ocean cores studied [*Bischof and Darby*, 1997].

4.5. Sequential Ice Sheet Collapses

[32] Over the last 34 kyr, large IRD events have occurred in sequence, first from the Innuitian Ice sheet and then from the Arctic Laurentide ice. This linkage suggests that one event might trigger another, as suggested earlier for ice sheets in general [*Andrews et al.*, 1998a]. More recently, on the basis of Sr-Nd fingerprints of the >150 μm IRD, *Grousset et al.* [2000] proposed that the Fennoscandian ice sheets began to collapse about 1.4 kyr before the eastern Laurentide ice sheets that produced the Heinrich events.

[33] The intriguing question of why the Innuitian Fe oxide peaks precede Arctic Laurentide collapse events might be found in the nature and scale of the Innuitian ice sheet versus the much larger Laurentide and Fennoscandian ice sheets. Because of its more northern location the Innuitian ice sheet began to grow sooner, and when isostatic depression overtook the global sea level drop, the Innuitian glaciers reached the sea and began to form floating margins, subsequently releasing icebergs (Figure 7). How this collapse and the corresponding sea level rise influenced the subsequent iceberg calving from the Arctic Laurentide Ice sheet is unknown. The effect of any sea level rise should be instantaneous instead of a thousand years later as suggested by the older IRD events (Table 2[1]). Chronological uncertainties do not allow a definitive determination of the time lag between IIS and ALIS events.

4.6. Correlation to North Atlantic Heinrich Events

[34] The discovery of Arctic ice export events through Fram Strait raises the question of their relationship to the Heinrich events. The definitive answer can only be found if an actual H layer is analyzed from the bottom upward for an

[1] Supporting data and data table are available via Web browser or via Anonymous FTP from ftp://kosmos.agu.org, directory "append" (Username = "anonymous", Password = "guest"); subdirectories in the ftp site are arranged by paper number. Information on searching and submitting electronic supplements is found at http://www.agu.org/pubs/esupp_about.html.

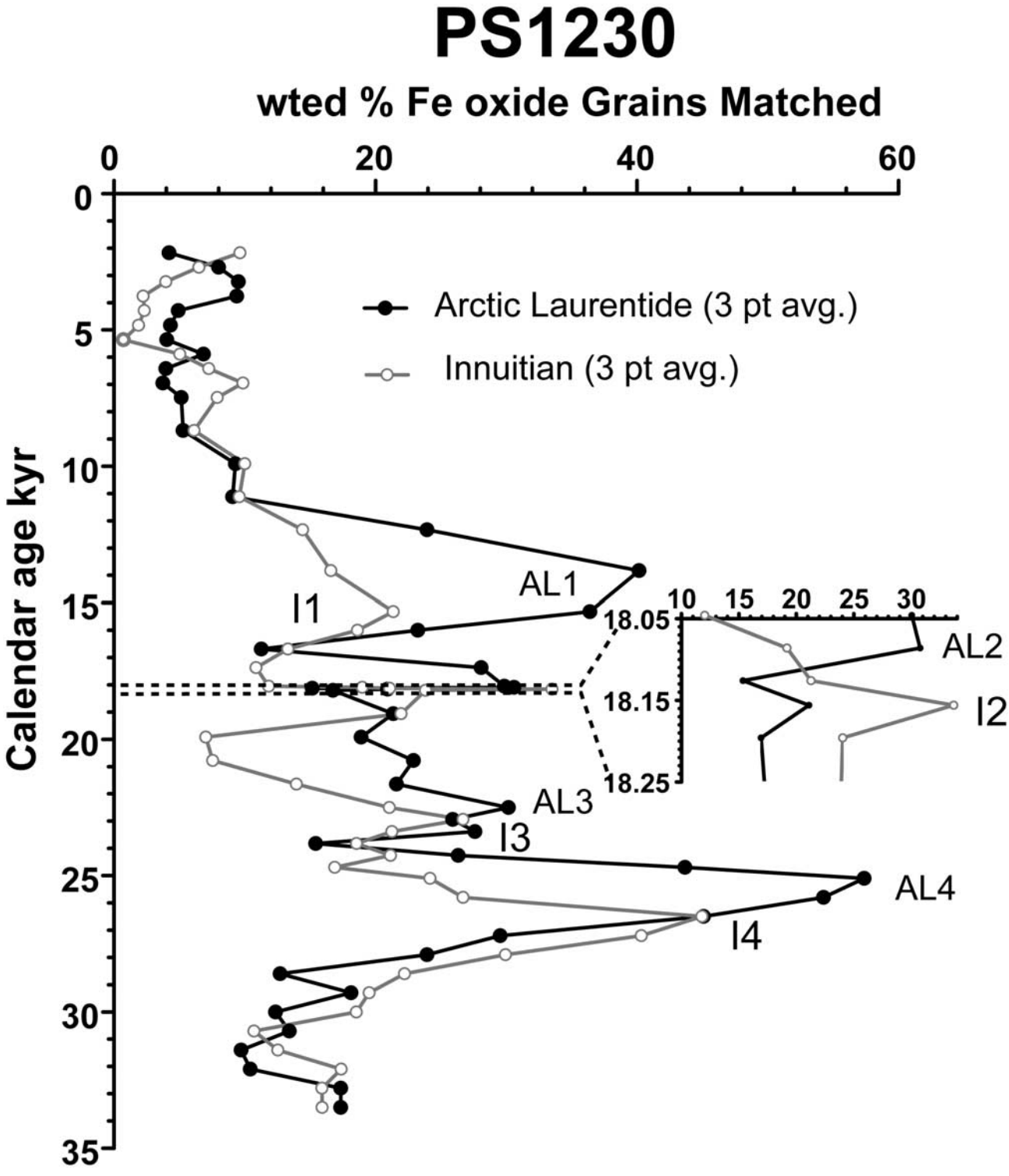

Figure 6. Innuitian IRD events more clearly shown leading Arctic Laurentide events in PS1230 when both curves are averaged over three sample intervals.

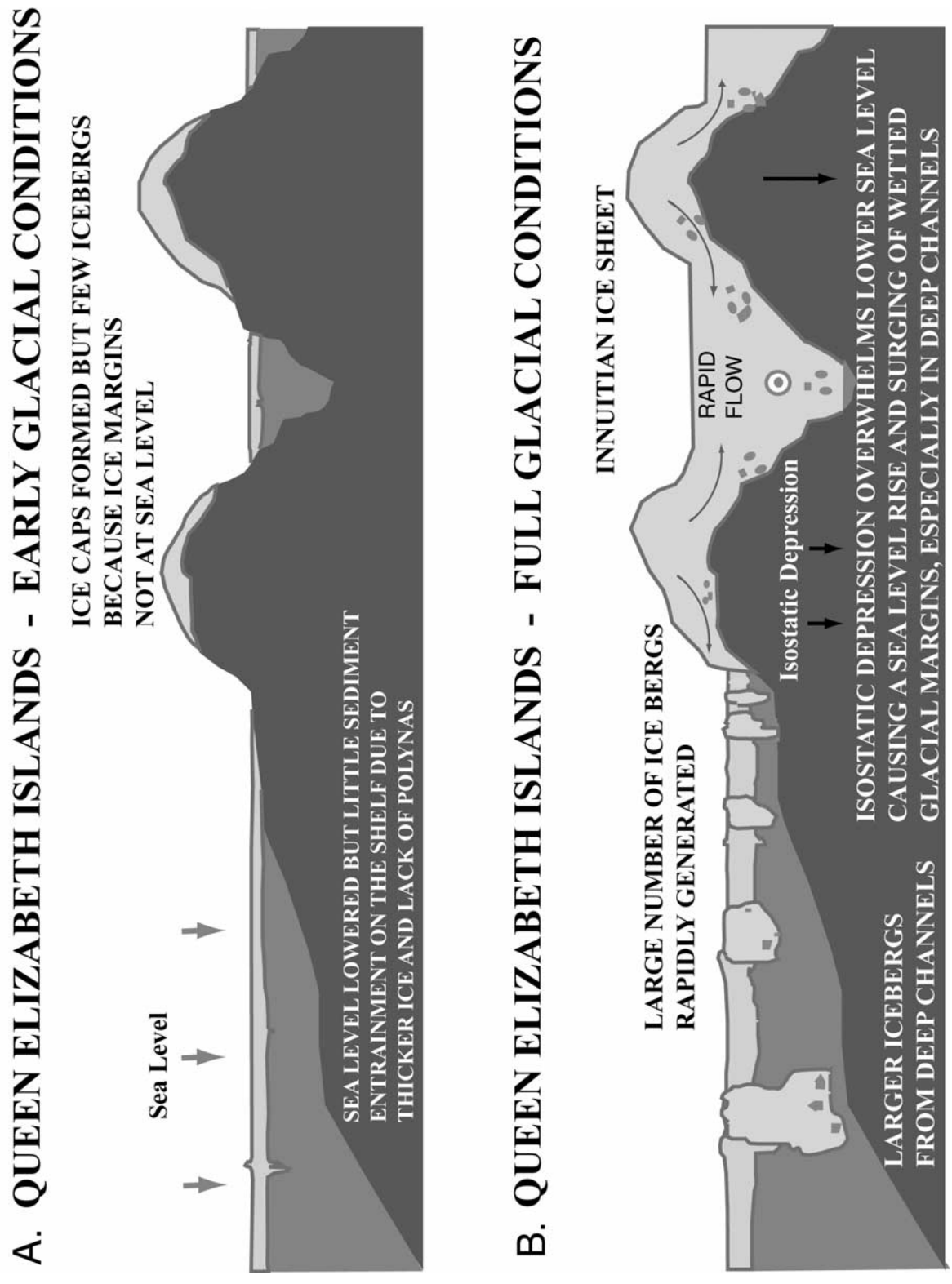

Figure 7. Diagram depicting the growth and decay of the Innuitian ice sheet on the Queen Elizabeth Islands west of Greenland. (a) Initial growth of ice caps on these islands and little to no icebergs produced. Sea ice entrainment is possible on the shallow shelf area. (b) Buildup of ice caps that have partially coalesced. The size of this ice sheet causes isostatic depression that brings sea level into contact with glacial margins and initiates a rapid disintegration of this ice sheet.

Table 2. Published Ages for North Atlantic Heinrich Events Compared to Those of Arctic Laurentide Events

	Radiocarbon Ages: North Atlantic Heinrich Events[a]			
	H-0 (n = 24)	H-1 (n = 44)	H-2 (n = 45)	H-3 (n = 24)
Mean	10,977	14,922	20,631	27,955
SD	743	1,260	1,400	1,577
Range	10,500–10,800	13,540–15000	18,240–23,780	25,260–30,950
	Radiocarbon Ages: Arctic Laurentide Ice Sheet Events			
	AL1	AL2	AL3	AL4
PS1230	12,780	15,740	20,120	30,340
92BC17	12,500	15,000		
94BC16	12,400	16,300	21,300	29,200
94BC28	13,810	15,160	24,460	
Mean	12,873	15,550	21,960	29,770
SD	645	593	2,244	806
Mean – SD	12,227	14,957	19,716	28,964
AL to H Event	1,896	628	1,329	1,815
	Calendar Ages: North Atlantic Heinrich Events			
	H-0 (n = 1)	H-1 (n = 3)	H-2 (n = 6)	H-3 (n = 3)
Mean	12,200	15,500	23,280	31,600
SD	0	500	1,910	1,010
Range	12,200	15,000–16,000	21,500–26,800	30,500–32,500
	Calendar Ages: Arctic Laurentide Ice Sheet Events			
	AL1	AL2	AL3	AL4
PS1230	15,320	18,220	23,860	34,370
92BC17	14,400	17,900		
94BC16	13,700	18,860	24,670	35,400
94BC28	14,100	18,100	27,000	
Mean	14,380	18,270	25,177	34,885
SD	689	415	1,630	728
Mean – SD	13,691	17,855	23,547	34,157
AL to H event	2,180	2,770	1,897	3,285

[a]References: *Andrews* [1998b, 2000], *Andrews and Tedesco* [1992], *Andrews et al.* [1998a, 1998d], *Bard et al.* [1987, 2000], *Baumann et al.* [1995], *Baas et al.* [1997], *Bond and Lotti* [1995], *Bond et al.* [1992, 1993, 1997, 1999], *Broecker et al.* [1992], *Dansgaard et al.* [1989], *Dowdeswell et al.* [1998], *Fronval et al.* [1995], *Grousset et al.* [2000], *Haflidason et al.* [1995], *Kirby* [1998], *McManus et al.* [1998], *Rochon et al.* [1998], *Stein et al.* [1996], *van Kreveld et al.* [1996], *Wang and Hesse* [1996], *Zahn et al.* [1997], and *Zhisheng and Porter* [1997]. For H event dates used, see supporting data and data table.

unambiguous succession of IRD grains from the IIS, then the ALIS, and then from Hudson Bay. Despite the large range of ages for the H events (Figure 8) and the low resolution of the Fram Strait and Arctic Ocean cores, some kind of relationship exists between the Arctic and North Atlantic IRD events. The number of ALIS events and their occurrence intervals over the last 34 kyr are remarkably similar to those of H events. AL1 appears to correspond to H-0 or the Younger Dryas and so forth for the other ALIS events.

[35] Although these Arctic ice export events occur at roughly the same times as Heinrich events in the North Atlantic, the average age of each ALIS event appears to precede the average age for each of the last four H events in the North Atlantic (Figure 8 and Table 2). While there is a large range of age dates for each of the H events in different cores, the ages of the ALIS events in the Arctic always occur at the older end of these H event ages (Figure 8). Even subtracting an additional 500 years for the reservoir correction from these arctic events as suggested by *Bard et al.* [1994] does not change the fact that they appear older than H events (Table 2). Larger reservoir age corrections of 0.8 to 1.5 kyr are suggested by *Waelbroeck et al.* [2001] due to the change in circulation with climate changes in higher latitudes (>40°N). Such corrections would eliminate much, if not all, of the lead time between ALIS events and Heinrich events, but more work is needed to determine when these reservoir age differences occur and what the correction would be for foraminifera living 24° farther north than the most northern core location used by *Waelbroeck et al.* [2001]. There is also the possibility that each ALIS event lags an earlier H event. However, this appears unlikely because H events lag ALIS events by a quarter to a third of the time interval between ALIS events and the preceding H event. Only AL1 is nearly halfway between the average age for H-1 and H-0, but then there is no ALIS event following H-0 as one would expect if ALIS events lagged H events.

[36] The timing between these events has important implications for ice sheet dynamics and the climate history. If there is a lead-lag relationship, then the Arctic Laurentide ice sheet may be disintegrating ~1.5 kyr (1.4 kyr ^{14}C and 1.7 kyr calendar) prior to the eastern Laurentide ice sheet that produced the H events (Table 2). This is remarkably similar to the lead time of precursor IRD events to H events [*Bond et al.*, 1999]. The period between IIS and ALIS events is also 1–2 kyr, or about the period of the cold peaks of the Dansgaard-Oeschger cycle or the IRD peaks of a Bond cycle [*Broecker et al.*, 1992; *Bond et al.*, 1999]. Not all of the ALIS and IIS

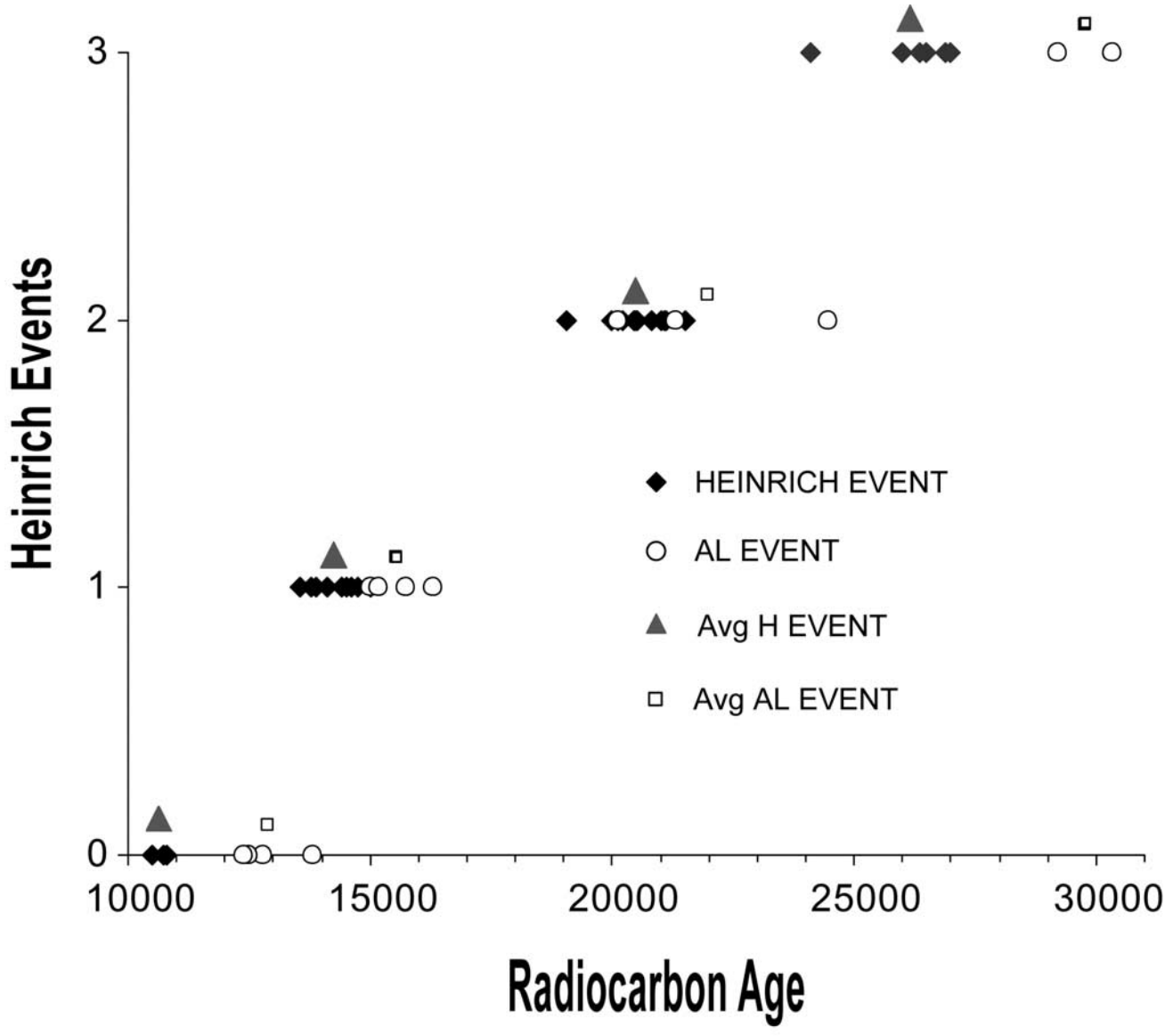

Figure 8. Plot of the published radiocarbon and calendar ages for each of the last four Heinrich events in the North Atlantic. Rather than convert published C dates to calendar ages, these dates are plotted separately for each type of age. The ages for each ALIS event from four Arctic cores including the Fram Strait core are also plotted along with averages in both the corrected radiocarbon format and the calibrated calendar age. The average age of H events based solely on detrital carbonate peaks is also shown because of the potential confusion over IRD peaks for H events and their precursor events.

events are 1.5 kyr apart in PS1230, but the sedimentation rates are not high enough to resolve these millennial-scale cycles. Obviously, higher-resolution cores are needed to resolve these potential relationships.

5. Conclusions

[37] The Fram Strait core records four ice-rafting events from the Arctic Laurentide ice sheet that represent large numbers of icebergs from the repeated collapse of this ice sheet into the Arctic Ocean. Some of these IRD events are also recorded in at least three other cores across the Arctic Ocean. Each of these IRD events is preceded by an IRD event from the Innuitian ice sheet. The lag time is not well constrained but is $\sim$1–2 kyr. Thus the Innuitian events immediately precede and possibly trigger a larger ALIS event. Each of these IRD events involved $\sim$0.5 million km^3 of ice from the ALIS plus smaller amounts of Innuitian ice. The icebergs drifted through Fram Strait into the Nordic seas and possibly reached the North Atlantic. While the relationship between these Arctic events and the larger H events of the North Atlantic is yet to be resolved, the Arctic

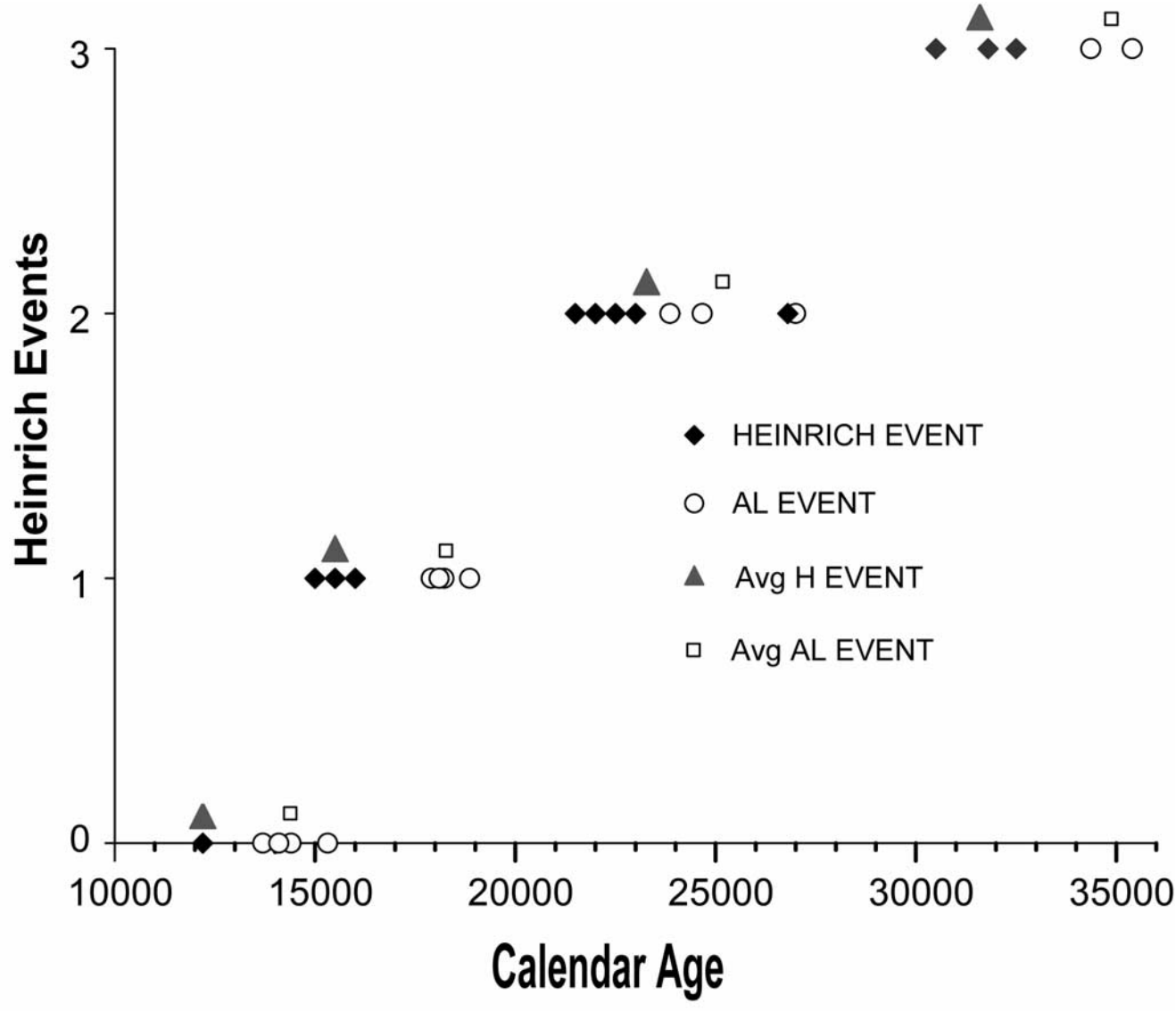

Figure 8. (continued)

seems to be responding to similar climate forcing resulting in similar periodicity.

[38] **Acknowledgments.** This work was supported by NSF grants OPP-9614451 and OPP-9817051. We acknowledge G. Bonani (ETH Zurich), J. Heinemeier (Aarhus University), and B. Kromer (Heidelberg University) and their staffs for the AMS radiocarbon analyses. Reviews of earlier drafts by G. Bond, R. Stein, S. Pfirman, and L. Polyak improved the manuscript, and we thank them for their comments. Source area samples were provided by S. Pfirman (Barnard College), A. Solheim (Norsk Polarinstitutt), J. England (University of Alberta), D. Forbes, B. MacLean, P. Mudie, G. Sonnichson, W. Blake Jr., J. Vincent, D. Lemmen, A. Dyke, D. Hodgson, and I. Hardy (Geological Survey of Canada), S. Lamoureux and R. Gilbert (Queenís University), S. Funder and C.E. Bøggild (Geological Survey of Greenland and Denmark), B. Conard (Oregon State University), and L. Hickey (Yale University).

References

Aagaard, K., and E. C. Carmack, The role of sea ice and other fresh water in the Arctic circulation, *J. Geophys. Res.*, *94*, 14,485–14,498, 1989.

Andrews, J. T., Dating glacial events and correlation to global climate change, in *Dating and Earthquakes: Review of Quaternary Geochronology and Its Application to Paleoseismology*, edited by J. M. Sowers, J. S. Noller, and W. R. Lettis, pp. 703–716, U. S. Nucl. Regulatory Comm., Off. of Nucl. Regulatory Res., Washington, D. C., 1998a.

Andrews, J., Abrupt changes (Heinrich events) in late Quaternary North Atlantic marine environments; a history and review of data and concepts, *J. Quat. Sci.*, *13*(1), 3–16, 1998b.

Andrews, J. T., Explained and unexplained spatial and temporal variability in rates of marine sediment accumulation along the northeast margin of the Laurentide ice sheet ≤14 ka, *J. Sed. Res.*, *70*, 782–787, 2000.

Andrews, J., and K. Tedesco, Detrital carbonate-rich sediments, northwestern Labrador Sea: Implications for ice-sheet dynamics and iceberg rafting (Heinrich) events in the North Atlantic, *Geology*, *20*, 1087–1090, 1992.

Andrews, J. T., T. A. Cooper, A. E. Jennings, A. B. Stein, and H. Erlenkeuser, Late Quaternary IRD events on the Denmark Strait/south-

east Greenland continental slope (~65°N): Related to North Atlantic Heinrich events?, *Mar. Geol.*, *149*, 211–228, 1998a.

Andrews, J., M. Kirby, A. Aksu, D. Barber, and D. Meese, Late Quaternary detrital carbonate (DC-) layers in Baffin Bay marine sediments (67°–74°N); correlation with Heinrich events in the North Atlantic, *Quat. Sci. Rev.*, *17*, 1125–1137, 1998b.

Baas, J., J. Mienert, F. Abrantes, and A. Prins, Late Quaternary sedimentation on the Portuguese continental margin: Climate-related processes and products, *Palaeogeogr. Palaeoclimatol. Palaeoecol.*, *130*(1–4), 1–23, 1997.

Bard, E., M. Arnold, P. Maurice, J. Duprat, J. Moyes, and J. C. Duplessy, Retreat velocity of the North Atlantic polar front during the last deglaciation determined by (super ^{14}C accelerator mass spectrometry), *Nature*, *328*, 791–794, 1987.

Bard, E., M. Arnold, J. Mangerud, M. Paterne, L. Labeyrie, J. Duprat, M. A. Melieres, and E. Sonstegaard, The North Atlantic atmospheric-sea surface ^{14}C gradient during the Younger Dryas climatic event, *Earth Planet. Sci. Lett.*, *126*, 275–287, 1994.

Bard, E., F. Rostek, J. L. Turon, and S. Gendreau, Hydrological impact of Heinrich events in the subtropical northeast Atlantic, *Science*, *289*, 1321–1324, 2000.

Bauch, H. A., H. Erlenkeuser, R. F. Spielhagen, U. Struck, J. Matthiessen, J. Thiede, and J. Heinemeier, A multiproxy reconstruction of the evolution of deep and surface waters in the subarctic Nordic seas over the last 30,000 years, *Quat. Sci. Rev.*, *20*, 659–678, 2001.

Baumann, K., K. Lackschewitz, J. Mangerud, R. Spielhagen, T. Wolf-Welling, R. Henrich, and H. Kassens, Reflection of Scandinavian ice sheet fluctuations in Norwegian Sea sediments during the past 150,000 years, *Quat. Res.*, *43*(2), 185–197, 1995.

Bischof, J. F., *Ice Drift, Ocean Circulation, and Climate Change*, 215 pp., Springer-Verlag, New York, 2000.

Bischof, J. F., and D. A. Darby, Mid to late Pleistocene ice drift in the western Arctic Ocean: Evidence for a different circulation in the past, *Science*, *277*, 74–78, 1997.

Bischof, J. F., and D. A. Darby, Quaternary ice transport in the Canadian Arctic and extent of late Wisconsinan glaciation in the Queen Elizabeth Islands, *Can. J. Earth Sci.*, *36*(12), 2007–2022, 1999.

Bischof, J. F., D. L. Clark, and J. S. Vincent, Pleistocene paleoceanography of the central Arctic Ocean: The sources of ice rafted debris and the compressed sedimentary record, *Paleoceanography*, *11*(6), 743–756, 1996.

Bond, G., and R. Lotti, Iceberg discharges into the North Atlantic on millennial time scales during the last glaciation, *Science*, *267*, 1005–1010, 1995.

Bond, G., et al., Evidence for massive discharges of icebergs into the North Atlantic Ocean during the last glacial period, *Nature*, *360*, 245–249, 1992.

Bond, G., W. Broecker, S. Johnsen, J. McManus, L. Labeyrie, J. Jouzel, and G. Bonani, Correlations between climate records from North Atlantic sediments and Greenland ice, *Nature*, *365*, 143–147, 1993.

Bond, G., W. Showers, M. Cheseby, R. Lotti, P. Almasi, P. deMenocal, P. Priore, H. Cullen, I. Hajdas, and G. Bonani, A pervasive millennial-scale cycle in North Atlantic Holocene and glacial climates, *Science*, *278*, 1257–1266, 1997.

Bond, G., W. Showers, M. Elliot, M. Evans, R. Lotti, I. Hajdas, G. Bonani, and S. Johnson, The North Atlantic's 1–2 kyr climate rhythm: Relation to Heinrich events, Dansgaard/Oeschger cycles, and the Little Ice Age, in *Mechanisms of Global Climate Change at Millennial Time Scales*, *Geophys. Monogr. Ser.*, vol. 112, edited by P. U. Clark, R. S. Webb, and L. D. Keigwin, pp. 35–58, AGU, Washington, D. C., 1999.

Broecker, W., G. Bond, M. Klas, E. Clark, and J. McManus, Origin of the northern Atlantic's Heinrich events, *Clim. Dyn.*, *6*(3–4), 265–273, 1992.

Clark, D. L., R. R. Whitman, K. A. Morgan, and S. D. Mackey, Stratigraphy and glacial-marine sediments of the Amerasian Basin, central Arctic Ocean, *Spec. Pap. Geol. Soc. Am.*, *181*, 57, 1980.

Clark, D. L., M. Andree, W. S. Broecker, A. C. Mix, G. Bonani, H. J. Hofmann, E. Morenzoni, M. Nessi, M. Suter, and W. Woelfli, Arctic Ocean chronology confirmed by accelerator ^{14}C dating, *Geophys. Res. Lett.*, *13*(4), 319–321, 1986.

Clark, P. U., J. M. Licciardi, D. R. MacAyeal, and J. W. Jenson, Numerical reconstruction of a soft-bedded Laurentide Ice sheet during the Last Glacial Maximum, *Geology*, *24*, 679–682, 1996.

Dansgaard, W., J. White, and S. Johnsen, The abrupt termination of the Younger Dryas climate event, *Nature*, *339*, 532–534, 1989.

Dansgaard, W., et al., Evidence for general instability of past climate from a 250-kyr ice-core record, *Nature*, *364*, 218–220, 1993.

Darby, D. A., and J. F. Bischof, A statistical approach to source determination of lithic and Fe oxide grains: An example from the Alpha Ridge Arctic Ocean, *J. Sed. Res.*, *66*, 599–607, 1996.

Darby, D. A., and J. F. Bischof, Evidence for the Chukchi Sea as an important source of sea-ice entrainment and the role of sea-ice in transporting fine-grained sediment from one shelf to another in the Arctic (abstract), *Eos Trans. AGU*, *79*(47), Fall Meet. Suppl. F31, 1998.

Darby, D. A., J. F. Bischof, and G. A. Jones, Radiocarbon chronology of depositional regimes in the western Arctic Ocean, *Deep Sea Res., Part II*, *44*, 1745–1757, 1997.

Dowdeswell, J. A., and E. K. Dowdeswell, Debris in icebergs and rates of glaci-marine sedimentation: Observations from Spitsbergen and a simple model, *J. Geol.*, *97*(2), 221–231, 1989.

Dowdeswell, J., and T. Murray, Modelling rates of sedimentation from icebergs, in Glacimarine Environments: Processes and Sediments, *Geol. Soc. Spec. Publ.*, *53*, 121–137, 1990.

Dowdeswell, J. A., M. A. Maslin, J. T. Andrews, and I. N. McCave, Iceberg production, debris rafting, and the extent and thickness of Heinrich layers (H-1, H-2) in North Atlantic sediments, *Geology*, *23*, 301–304, 1995.

Dowdeswell, J. A., A. Elverhoi, and R. Spielhagen, Glaciomarine sedimentary processes and facies on the polar North Atlantic margins, *Quat. Sci. Rev.*, *17*, 243–272, 1998.

Dyke, A. S., A reinterpretation of glacial and marine limits around the northwestern Laurentide Ice sheet, *Can. J. Earth Sci.*, *24*(4), 591–601, 1987.

Dyke, A. S., Last Glacial Maximum and deglaciation of Devon Island, Arctic Canada: Support for an Innuitian ice sheet, *Quat. Sci. Rev.*, *18*, 393–420, 1999.

Dyke, A. S., J. S. Vincent, J. T. Andrews, L. A. Dredge, and W. R. Cowan, The Laurentide Ice sheet and an introduction to the Quaternary geology of the Canadian Shield, in *The Geology of North America*, vol. K-1, *Quaternary Geology of Canada and Greenland*, edited by R. J. Fulton, pp. 178–189, Geol. Soc. of Am., Boulder, Colo., 1989.

Dyke, A. S., T. F. Morris, D. E. C. Green, and J. England, Quaternary geology of Prince of Wales Island Arctic Canada, *Geol. Surv. Can. Mem.*, *433*, 142 pp., 1992.

England, J., Coalescent Greenland and Innuitian ice during the Last Glacial Maximum: Revising the Quaternary of the Canadian High Arctic, *Quat. Sci. Rev.*, *18*(3), 421–456, 1999.

Escher, A., and W. S. Watt (Eds.), *Geology of Greenland*, 603 pp., *Groenlands Geol. Unders.*, Copenhagen, Denmark, 1976.

Fronval, T., E. Jansen, J. Bleomendal, and S. Johnsen, Oceanic evidence for coherent fluctuations in Fennoscandian and Laurentide ice sheets on millennium timescales, *Nature*, *374*, 443–446, 1995.

Grousset, F. E., C. Pujol, L. Labeyrie, G. Auffret, and A. Boelaert, Were the North Atlantic events triggered by the behavior of the European ice sheets?, *Geology*, *28*, 123–126, 2000.

Haflidason, H., H. Sejrup, D. Kristensen, and S. Johnsen, Coupled response of the late glacial climatic shifts of northwest Europe reflected in Greenland ice cores; evidence from the northern North Sea, *Geology*, *23*, 1059–1062, 1995.

Hebbeln, D., and G. Wefer, Effects of ice coverage and ice-rafted material on sedimentation in the Fram Strait, *Nature*, *350*, 409–411, 1991.

Henrich, R., H. Kassens, E. Vogelsang, and J. Thiede, Sedimentary facies of glacial-interglacial cycles in the Norwegian Sea during the last 350 ka., *Mar. Geol.*, *86*, 83–319, 1989.

Jones, G. A., and L. Keigwin, Evidence from Fram Strait (78°N) for early deglaciation, *Nature*, *336*, 56–59, 1988.

Kirby, M., Heinrich event-0 (DC-0) in sediment cores from the northwest Labrador Sea; recording events in Cumberland Sound?, *Can. J. Earth Sci.*, *35*(5), 510–519, 1998.

Kwok, R., and D. A. Rothrock, Variability of Fram Strait ice flux and North Atlantic Oscillation, *J. Geophys. Res.*, *104*, 5177–5189, 1999.

MacAyeal, D. R., Binge/purge oscillations of the Laurentide Ice sheet as a cause of the North Atlantic Heinrich events, *Paleoceanography*, *8*(6), 775–784, 1993.

McManus, J. F., R. F. Anderson, W. S. Broecker, M. Q. Fleisher, and S. M. Higgins, Radiometrically determined sedimentary fluxes in the sub-polar North Atlantic during the last 140,000 years, *Earth Planet. Sci. Lett.*, *155* (1–2), 29–43, 1998.

Mysak, L. A., and S. A. Venegas, Decadal climate oscillations in the Arctic: A new feedback loop for atmosphere-ice-ocean interactions, *Geophys. Res. Lett.*, *25*(19), 3607–3610, 1998.

Nürnberg, D., I. Wollenburg, D. Dethleff, H. Eicken, H. Kassens, T. Letzig, E. Reimnitz, and J. Theide, Sediments in Arctic sea ice: Implications for entrainment, transport and release, *Mar. Geol.*, *119*, 185–214, 1994.

O'Cofaigh, C., J. England, and M. Zreda, Late Wisconsinan glaciation of southern Eureka Sound: Evidence for extensive Innuitian ice in the Canadian High Arctic during the Last Glacial Maximum, *Quat. Sci. Rev.*, *19*, 1319–1341, 2000.

Okulitch, A. V., B. G. Lopatin, and H. R. Jackson, Circumpolar geologic map of the Arctic, *Geol. Surv. Can. Map*, *1765 A*, scale 1:6.000.000, 1989.

Oppo, D. W., and S. J. Lehman, Suborbital timescale variability of North Atlantic Deep Water during the past 200,000 years, *Paleoceanography*, *10*(5), 901–910, 1995.

Pfirman, S., A. Abelmann, J. C. Gascard, I. Wollenburg, and P. Mudie, Particle-laden Eurasian Arctic sea ice: Observations from July and August 1987, *Polar Res.*, *7*(1), 59–66, 1989.

Polyak, L., M. H. Edwards, B. J. Coakley, and M. Jakobsson, Ice shelves in the Pleistocene Arctic Ocean inferred from glaciogenic deep-sea bedforms, *Nature*, *410*, 453–457, 2001.

Poore, R. Z., L. Osterman, W. B. Curry, and R. L. Phillips, Late Pleistocene and Holocene meltwater events in the western Arctic Ocean, *Geology*, *27*, 759–762, 1999.

Reimnitz, E., E. W. Kempema, and P. W. Barnes, Anchor ice, seabed freezing, and sediment dynamics in shallow Arctic seas, *J. Geophys. Res.*, *92*, 14,671–14,678, 1987.

Reimnitz, E., M. McCormick, J. Bischof, and D. Darby, Comparing sea-ice sediment load with Beaufort Sea shelf deposits: Is entrainment selective?, *J. Sed. Res.*, *68*, 777–787, 1998.

Rochon, A., A. de Vernal, H. P. Sejrup, and H. Haflidason, Palynological evidence of climate and oceanographic changes in the North Sea during the last deglaciation, *Quat. Res.*, *49*(2), 197–207, 1998.

Ruddiman, W. F., Late Quaternary deposition of ice-rafted sand in the sub-Arctic North Atlantic (lat. 40° to 65°N), *Geol. Soc. Am. Bull.*, *88*, 1813–1827, 1977.

Stein, R., C. Schubert, C. Vogt, and D. K. Futterer, Stable isotope stratigraphy, sedimentation rates, and salinity changes in the latest Pleistocene to Holocene central Arctic Ocean, *Mar. Geol.*, *119*, 333–355, 1994.

Stein, R., N. Seung-Il, H. Grobe, and H. Hubberten, Late Quaternary glacial history and short-term ice-rafted debris fluctuations along the east Greenland continental margin, in *Late Quaternary Palaeoceanography of the North Atlantic Margins*, edited by J. Andrews et al., *Geol. Soc. Spec. Publ., 111*, 135–151, 1996.

Stuiver, M., and P. J. Reimer, Extended ^{14}C data base and revised CALIB 3.0 ^{14}C age calibration program, *Radiocarbon*, *35*, 215–230, 1993.

Stuiver, M., P. J. Reimer, E. Bard, J. W. Beck, G. S. Burr, K. A. Hughen, B. Kromer, G. McCormack, J. van der Plicht, and M. Spurk, INTCAL98 radiocarbon age calibration, 24,000-0 cal BP, *Radiocarbon*, *40*, 1041–1083, 1998.

van Kreveld, S., M. Knappertsbusch, J. Ottens, G. Ganssen, and J. van Hinte, Biogenic carbonate and ice-rafted debris (Heinrich layer) accumulation in deep-sea sediments from a Northeast Atlantic piston core, *Mar. Geol.*, *131*(1–2), 21–46, 1996.

Voelker, A. H. L., M. Sarnthein, P. M. Grootes, H. Erlenkeuser, C. Laj, A. Mazaud, M. J. Nadeau, and M. Schleicher, Correlation of marine ^{14}C ages from the Nordic Seas with the GISP2 isotope record: Implications for ^{14}C calibration beyond 25 ka BP, *Radiocarbon*, *40*(1), 517–534, 1998.

Wang, D., and R. Hesse, Continental slope sedimentation adjacent to an ice-margin, II, Glaciomarine depositional facies on Labrador slope and glacial cycles, *Mar. Geol.*, *135*(1–4), 65–96, 1996.

Waelbroeck, C., J.-C. Duplessy, E. Michel, L. Labeyrie, D. Paillard, and J. Duprat, The timing of the last deglaciation in North Atlantic climate records, *Nature*, *412*, 724–726, 2001.

Warren, C. R., Iceberg calving and the glacioclimatic record, *Prog. Phys. Geogr.*, *16*(3), 253–282, 1992.

Zahn, R., H. Erlenkeuser, P. Grootes, J. Schonfeld, H. R. Kudrass, and P. Myong-Ho, Thermohaline instability in the North Atlantic during meltwater events: Stable isotope and ice-rafted detritus records from core, *Paleoceanography*, *12*(5), 696–710, 1997.

Zhisheng, A., and S. C. Porter, Millennial-scale climatic oscillations during the last interglaciation in central China, *Geology*, *25*, 603–606, 1997.

J. F. Bischof, D. A. Darby, S. W. Herman, and S. A. Marshall, Department of Ocean, Earth, and Atmospheric Sciences, Old Dominion University, Norfolk, VA 23529, USA. (ddarby@odu.edu)

R. F. Spielhagen, GEOMAR Research Center for Marine Geosciences, Wischhofstrasse 1–3, D-24148, Kiel, Germany.